

RSC Advances



This is an *Accepted Manuscript*, which has been through the Royal Society of Chemistry peer review process and has been accepted for publication.

Accepted Manuscripts are published online shortly after acceptance, before technical editing, formatting and proof reading. Using this free service, authors can make their results available to the community, in citable form, before we publish the edited article. This *Accepted Manuscript* will be replaced by the edited, formatted and paginated article as soon as this is available.

You can find more information about *Accepted Manuscripts* in the [Information for Authors](#).

Please note that technical editing may introduce minor changes to the text and/or graphics, which may alter content. The journal's standard [Terms & Conditions](#) and the [Ethical guidelines](#) still apply. In no event shall the Royal Society of Chemistry be held responsible for any errors or omissions in this *Accepted Manuscript* or any consequences arising from the use of any information it contains.



Journal Name

ARTICLE

Ti-decorated boron monolayer: A promising material for hydrogen storage

Received 00th January 20xx,
Accepted 00th January 20xx

DOI: 10.1039/x0xx00000x

www.rsc.org/

FuChun Zhang,^a Rui Chen,^b and Weihu Zhang,^c and WeiBin Zhang,^{a†}

A promising Ti-decorated boron monolayer (BM) system for hydrogen storage is proposed through the use of density functional theory. We find that the Ti decoration on BM system is more stable, and the charge transfer between atoms will induce in a more active system. The thermodynamic analysis showed that the doped Ti atoms reduced the thermodynamic stability of BM sheets, but suitable for hydrogen storage system. One Ti atom-decorated BM can adsorb up to 5 H₂ molecules, and the orbital interaction is mainly due to H 1s, Ti 3d and B 1 2p orbital hybridization. The LST/QST calculation shows that the cluster formation can be excluded due to the high energy barrier. Therefore, 16Ti atoms can be decorated on the double faces of the H1_t positions and corresponding capacity of the system for H₂ storage is calculated to be about 10.44 wt %. Our results suggest that the Ti-BM will be a promising material system for hydrogen storage.

1. Introduction

Hydrogen has been recognized as an attractive energy carrier, as it provides renewable and clean energy source, and is abundantly present in nature. However, the application of H₂ is still limited as the great challenge of transportation and efficiency of storage. Hydrogen storage in solid-state materials has been attracting a wide range of interests. For the past decade, metal or chemical hydride materials have been considered as a hydrogen storage medium. But, these materials have common shortcoming, like slow kinetics and poor reversibility^{1, 2}. Recently, carbon-based materials have been explored as a hydrogen storage medium because of the possibility of good reversibility, fast kinetics, and high capacity (large surface area)³⁻⁵. However, the storage capacity in these materials is significantly decreased at room temperature and

ambient pressure^{6, 7}, because the binding energy of H₂ is low and the possible clustering problem of the decorated materials. Boron is the nearest neighbor of carbon at the left of Periodic Table. Carbon's natural ground state structure is graphite, and the monolayer is the well-known graphene. However, the boron tends to form net-works of icosahedral clusters, not planar sheets. Recently, Sohrab Ismail-Beigi et al.⁸ performed theoretical calculations on a new class of two-dimensional boron sheets and found a sheet that is lower in energy than any structures previously considered. Xiaojun Wu et al.⁹ have reported that the β_1 boron monolayer (BM) is the most stable structure in all the heterostructures, and speculated the BM sheets may find applications such as specialized electrode in batteries or as lithium storage. Inspired by their work, the BM may be a promising hydrogen storage media due to their low weight and large specific surface area. Noteworthy, the BM is a typically porous structure, which can provide a patterned decorating/doping structure that can greatly enhance the capacity of hydrogen storage.

The light transition-metal atoms, such as Sc, Ti, and Co, are widely applied to be decorated on various kinds of hydrogen storage materials. Previous experimental¹⁰ and theoretical¹¹

^a College of physics and electronic information, Yan'an University, Yan'an 716000, P. R. China

^b Department of Chemistry, Hanyang University, Seoul 133791, Republic of Korea.

^c Communication and information engineering College, Xi'an University of Science and Technology, Xi'an 710054

†Corresponding author: Weibin Zhang, Email: zly512@163.com.

DOI: 10.1039/x0xx00000x

results show that Ti atoms covered on the carbon nanotubes can improve the hydrogen storage capacity. The decoration of Ti on SiC monolayer can lead to 5.0 wt% H₂ storage capacity¹². Ti-decorated boron-carbon-nitride monolayer and graphene can even store up to 7.6 wt% and 7.8 wt% in H₂ molecular form, respectively^{13,14}. Inspired by those previous reports, Ti-decorated BM may lead to a high hydrogen capacity. Therefore, further investigations about hydrogen storage with this Ti decorated θ_1 BM are desirable.

In this paper, we carry out a study on hydrogen storage properties of Ti-decorated BM (Ti/BM) by using density functional theory. The interactions of both Ti-decorating on BM and H₂ adsorption on Ti/BM were analyzed by computing charge population, projected electronic density of states, and electron density distribution. The Ti clustering problem was investigated by calculating the diffusion energy barriers at the transition state of Ti decorated atoms on the diffusion pathway. We concluded that the Ti-decorated BM will be a promising material for hydrogen storage applications.

2. Computational details

The DFT calculations were performed using the DMOL3code¹⁵. The generalized gradient approximation (GGA) with Perdew–Burke–Ernzerhof (PBE) function was employed as the exchange–correlation function¹⁶. A double numerical plus polarization basis set (DNP) was employed to expand the Kahn–Sham electronic eigen states with an orbital cutoff radius of 4.4 Å. The energy convergence tolerance was taken to be 2×10^{-5} Ha (1 Ha= 27.21 eV) with the allowed maximum force of 0.002 Ha/Å and displacement of 0.005 Å. The reciprocal space was represented via a Monkhorst–Pack special *k*-point scheme with $6 \times 6 \times 1$ *k*-points for structural optimization and electronic structure calculations. We considered boron monolayer with the vacuum width of 30 Å as a computational model system. H₂ molecule was optimized in a large periodic cubic box with a cell parameter of $10 \times 10 \times 10$ Å³ with H–H bond length of ~ 0.75 Å.

To investigate the possible clustering problem of Ti atoms on the BM, we performed the linear synchronous transition/quadratic synchronous transit (LST/QST)¹⁷ calculation in the DMOL3 code. Those methodologies have

been demonstrated as fantastic tools to search for the structure of the transition state (TS) and the minimum energy pathway. The diffusion energy barrier of Ti atom was defined as the difference between the energy at the TS and that at initial state (before diffusion to the neighboring sites) of the Ti/BM system.

In order to evaluate the possibility of cluster formation and the stability of the BM sheet after Ti doping, the thermodynamic calculations were performed. The thermodynamic parameters, including the enthalpy *H*, Gibbs free energy *G*, entropy *S* and heat capacity *C_p* were calculated at constant pressure. The calculation formula was shown below^{18,19}:

$$E(T) = E_{vib}(T) + E_{rot}(T) + E_{tra}(T) + RT \quad (1)$$

where the subscripts stand for vibration, rotational, and translational contributions, respectively, and *R* is the idea gas constant. For enthalpy correction *H*, the contributions are given by:

$$H_{vib} = \frac{R}{k} \frac{1}{2} \sum_i h\nu_i + \frac{R}{k} \sum_i \frac{h\nu_i \exp(-h\nu_i/kT)}{[1 - \exp(-h\nu_i/kT)]} \quad (2)$$

$$H_{rot}(linear) = RT \quad (3)$$

$$H_{rot}(nonlinear) = \frac{3}{2} RT \quad (4)$$

$$H_{tra} = \frac{3}{2} RT \quad (5)$$

For entropy *S*, the contributions are given by :

$$S_{vib} = R \sum_i \frac{h\nu_i/kT \exp(-h\nu_i/kT)}{1 - \exp(-h\nu_i/kT)} - R \sum_i \ln[1 - \exp(-h\nu_i/kT)] \quad (6)$$

$$S_{rot}(linear) = R \ln \left[\frac{8\pi^2 I k T}{\sigma h^2} \right] + R \quad (7)$$

$$S_{rot}(nonlinear) = \frac{R}{2} \ln \left[\frac{\pi}{\sqrt{\sigma}} \frac{8\pi^2 c I_A}{h} \frac{8\pi^2 c I_B}{h} \frac{8\pi^2 c I_C}{h} \left(\frac{kT}{hc} \right)^3 \right] + \frac{3}{2} R \quad (8)$$

$$S_{tra} = \frac{5}{2} R \ln T + \frac{3}{2} R \ln w + R \ln p - 2.31482 \quad (9)$$

As for heat capacity *C_p*, the contribution are given by:

$$C_{vib} = R \sum_i \frac{(h\nu_i/kT)^2 \exp(-h\nu_i/kT)}{[1 - \exp(-h\nu_i/kT)]^2} \quad (10)$$

$$C_{rot}(linear) = R \quad (11)$$

$$C_{rot}(nonlinear) = \frac{3}{2} R \quad (12)$$

$$C_{vra} = \frac{5}{2}R \quad (13)$$

In the above formulas, k is Boltzmann's constant, h is Planck's constant, ν_i is the individual vibrational frequencies, w is the molecular weight, I_x is the moment of inertia about axis x , and σ is the symmetry number.

3. Results and discussion

3.1 Decoration of Ti atoms on boron monolayer

When we considered the possible decoration sites of the Ti atom on BM, there are five different sites for Ti decoration on BM: the top of hexagonal rings ($H1_t$), the top of B1 atoms ($B1_t$), the top of B2 atoms ($B2_t$), the top of bridge sites between B1 atoms (B_{r1}) and the top of bridge sites between B1 and B2 atoms (B_{r2}), as shown in Fig 1. There are two kinds of B atoms: the first kind is the B atoms in the hexagonal rings (B1), which are surrounded by 5 neighboring B atoms; the second kind is B atoms surrounded by six neighboring B atoms (B2). Adsorption energy of the Ti atom adsorbed on $H1_t$, $B1_t$, $B2_t$, B_{r1} and B_{r2} sites were calculated to be -4.37, -4.15, -4.13, -4.03 and -3.98 eV, respectively. Thus, the Ti atom prefers to reside over the $H1_t$ position, which is the most stable position.

After finding the stable decoration site of Ti atom, we investigated the charge transfer between Ti and B atoms by calculating the charge population, as shown in Table 1. To be noted that the charge population of the system represents the charge transfer between atoms. The values of charge in the pristine BM are -0.05 and 0.16/ e /for B1 and B2 atoms, respectively. Ti decoration on BM leads to significant modification of the charge populations of B atoms on the monolayer. The negative charge on every B1 atoms around Ti atom increased to be -0.01/ e /, while the B2 atoms increased to be 0.28/ e . The charge on the Ti atom was 0.54/ e / after Ti decorating. As a result, the atoms in the Ti/BM system became more active. Moreover, the positive charge accumulation around Ti atoms induced an electrostatic field, which probably enhances the adsorption ability of H_2 molecules.

Fig. 2 shows the thermodynamic properties of pristine BM sheet and Ti-doped BM. In all cases, S , C_p and H increased gradually with the temperature increased, while G decreased with the temperature increased. At the same time, the thermodynamic property was also affected greatly by the Ti doping concentration. The S , C_p and H increased quickly with the increase of Ti doping concentration, while G value decreased slowly with increased Ti doping amount. This result indicates that doped Ti atom can weaken the thermodynamic stability of boron monolayer sheet. The higher the Ti doping concentration, the more unstable the BM. But, all the Ti doped BM system is stable as the G is positive below 600 K. Therefore, the Ti doped BM is stable and can be applied for hydrogen storage.

3.2. H_2 adsorption and desorption on Ti-decorated BM

Firstly, we investigated single H_2 adsorption and interaction with the Ti/BM. The adsorption sites of H_2 on Ti/BM were considered. As the H_2 adsorption originates due to the electrostatic field around the Ti atom, H_2 were mainly adsorbed around the top of Ti. The calculated adsorption energy of the H_2 adsorbed around the Ti atom is similar (around -0.47 eV/ H_2). After H_2 adsorption, the adsorption energy range is -0.47 eV/ H_2 , and the H-H bond length is 0.81 Å, as tabulated in Table 3. Noting that the bond length of the adsorbed H_2 increases to 0.82 Å compared with the original bond length of 0.75 Å. This phenomenon can be explained by the following process. As the electric field exists around the positive charged Ti, H_2 is polarized and approaches Ti. H_2 interacts with Ti to accept some positive charge from Ti/BM. Then, the additional positive charge in H_2 will enhance the repulsion interaction between the positive charges. Consequently, the H_2 bond is elongated.

The interaction between atoms can also be intuitively verified by analysis of the electron density distribution. Fig 3 illustrates the electron density distribution of the Ti/BM systems before and after H_2 adsorption. The blue regions represent electron deletion, while the red regions represent electron enrichment. The white regions mean that the electron density does not change obviously. Before H_2 adsorption, the electrons mainly existed in the regions between B and Ti atoms, as shown in Fig 3(a). After H_2 adsorption, some electron distribution was found in the

regions between H and Ti atoms (Fig. 3(b)), indicating the adsorption of H₂ on Ti/BM was weak chemisorption. It was worthwhile to note that the interaction between H₂ and Ti/BM mainly took place between H₂ and Ti atoms. The adsorbed H₂ molecules tended to tilt toward the Ti atoms because of charge redistribution.

To investigate the orbital interaction between H₂ molecules and Ti/BM, we analyzed the projected electronic density of state (PDOS) of the H₂-adsorbed Ti/BM system. Fig. 4 displays the PDOSs of H, Ti and B atoms before and after H₂ adsorption on the Ti/BM. Before H₂ adsorption, there is a hybridization area in PDOS among Ti 3*d*, B1 2*p*, and B2 2*p* orbital at ranging of -1.60 and 2.60 eV (dotted lines in Fig. 4(a)). After H₂ adsorbed on the Ti/BM, there are two new peaks of Ti 3*d* at 0.20 eV and -9.01 eV, which is due to the hybridization between Ti 3*d* and H 1*s*, as shown in Fig. 4(b). At the same time, there is a resonance between the H and Ti, B1 and B2 atoms at -9.01 eV. Those results suggest that Ti interacts with both H₂ and BM, and plays an important role for hydrogen storage. After electrostatic adsorption of H₂, charge transfer between atoms and orbital hybridization take place and form a more stable adsorption system. Therefore, H₂ adsorption on Ti/BM is suggestive of weak chemisorption, which is consistent with the results deduced from adsorption energy analysis.

Secondly, we investigated how many H₂ molecules can be adsorbed on one Ti decorated BM. We constructed an adsorption configuration with more than a single H₂ molecule adsorbed on the different positions. Table 2 tabulates the adsorption energies (E_a) and charge population of H₂ with different molecule adsorption numbers. As the number of the adsorbed H₂ molecules increased, E_a changed in the range from -0.20 to -0.47 eV/H₂. It is known that the ideal E_a between the host material and adsorbed H₂ molecules should be intermediate between physisorption and chemisorption energy (weak chemisorption), ranging from -0.20 to -0.80 eV. It was noted that a single Ti atom decorated on the B monolayer can adsorb up to 5 H₂ molecules with adsorption energy -0.20 eV/H₂, which is in the range of ideal adsorption energy levels. The bond length of the fifth H₂ is 0.79 Å and the charge on the molecule is -0.02/*e*, which means that the fifth H₂ is polarized and adsorbed around Ti. At the same time, the charge on the fifth H₂ changed from positive to negative,

indicating that the electron back donation occurred. H₂ molecules are distributed almost symmetrically around Ti atoms. Similar phenomena were observed on graphene decorated with rare earth elements (Y, Eu)^{21, 22}. The sixth H₂ escaped without forming a bond with Ti which could be explained as the interaction between H₂ would weaken the adsorption and the electron back donation will decrease the Coulomb force between Ti and H atoms. Therefore, the saturated number of H₂ adsorption is 5.

After thoroughly understanding the adsorption behavior of H₂ on one Ti atom decorated BM, we turn to adjusting the number of decorated Ti atoms to evaluate the maximum hydrogen storage ability of this system. The possible clustering problem of metal atoms adsorbed on supports (such as graphene, silylene) is a typical bottleneck for many proposed hydrogen storage materials. Thus, we carefully computed the energy barrier for Ti diffusion on the BM. Firstly, we consider one Ti atom migrating from aH1_t position to its nearest neighboring one. The atomic structures of the initial state (IS), the transition state (TS) and the final state (FS) during Ti atom migration are shown in Fig 5(a). We can calculate the diffusion energy barrier, $E_{bar} = E_{TS} - E_{IS}$, where E_{TS} and E_{IS} are the energies of the TS and the IS, respectively. Regarding TS, after the bonds between Ti and the surrounding B atoms are broken, Ti atom can diffuse and reach to the top of the B_{r1} (TS site) between two H1_t sites. Eventually, Ti can diffuse to the neighboring H1_t site, and then forms bonds with the B atoms on that site. The energy barrier, E_{bar} , of Ti for diffusing from the H1_t to its neighboring one on the BM is calculated to be 1.40 eV. Noting that, the distance between two Ti atoms in the nearest H1_t site is 2.58 Å, which is smaller than the distance between Ti atoms in Ti metal phase (~2.80 Å). Therefore, a Ti dimer formed between two nearest neighboring Ti atoms. But, the structure will be more stable as the adsorption energy and energy barrier are doubled due to the special dimer structure. On the other hand, we consider one Ti atom migrating from the H1_t position to its secondary nearest neighboring H1_t position, as shown in Fig 5(b). The E_{bar} of Ti for diffusing from H1_t to its neighboring one on the BM is calculated to be 2.75 eV, indicating the migrating in this pathway is very difficult. Therefore, it is difficult to form cluster on pristine BM. 16Ti atoms can be decorated on the

double faces of H_{1t} positions in the θ_1 BM with a value of $\eta=1/8$, as shown in Fig 6 (a). η is the global density parameter, which is defined as the ratio of number of hexagon holes to the number of atomic sites in the pristine triangular sheet within a unit cell of the decorated boron sheet⁹. In this particular geometry, ten H_2 can be adsorbed around every Ti dimer, as shown in Fig 6 (b). Eventually, 80 H_2 molecules could be adsorbed on the 1/8-boron monolayer system and corresponding capacity of the system for H_2 storage is calculated to be about 10.44 wt %. Jiling Li et al²³ have reported Li decorated BM for reversible hydrogen storage, corresponding to a hydrogen uptake of 15.26 wt %. Comparing with their work, we all choose the most stable boron monolayer (1/8-boron monolayer) and meet the hydrogen storage capacity target of DOE (9.0 wt %). But, there are many differences between our works. In their report, the binding energy of Li on BM is 2.18 eV/Li, which is a little higher than the cohesive energy of bulk Li (1.63 eV/Li). In our work, the adsorption energy of one Ti decorated on BM is -4.37 eV. Noteworthy, a Ti dimer formed between two nearest neighboring Ti atoms, which means the adsorption energy is double. The Ti decorated BM system is more stable than the Li decorated BM case. On the other hand, one Li decorated BM can adsorb 4 H_2 , while there are 5 H_2 can adsorb around each Ti atom. The positive charge on Li is less than 0.10 $|e|$, while the charge on Ti decreased from 0.54 to -0.39 $|e|$. The hydrogen adsorption ability of each Ti is obviously higher than the Li case.

4. Conclusions

In conclusion, the adsorption behavior of H_2 molecules on the Ti/BM system was studied by using density functional theory. We find that the Ti decoration on BM system to be stable with an adsorption energy of -4.37 eV. The thermodynamic analysis showed that the doped Ti atoms reduced the thermodynamic stability of BM sheets, but the Ti doped BM system is suitable for hydrogen storage system. The charges transfer between atoms, which make the atoms in the Ti/BM system become more active. One Ti atom-decorated BM can adsorb up to 5 H_2 molecules with the adsorption energies from -0.20 to -0.47 eV/ H_2 . The orbital interaction exists mainly between H_2 , Ti, and

B1, which is mainly due to H 1s, Ti 3d and B1 2p orbital hybridization. Then, the possible clustering problems were investigated with LST/QST calculation. The energy barrier of one Ti atom migrating from the H_{1t} position to its nearest neighboring H_{1t} position is 1.40 eV. But, a Ti dimer formed between two nearest neighboring Ti atoms, and the adsorption energy and diffusion energy barrier are doubled due to the special dimer structure. The energy barrier of one Ti atom migrating from the H_{1t} position to its secondary nearest neighboring H_{1t} position is 2.75 eV. The cluster formation can be vigorously excluded due to the high energy barrier. Therefore, 16Ti atoms can be decorated on the double faces of the H_{1t} positions and corresponding capacity of the system for H_2 storage is calculated to be about 10.44wt %. We can conclude that Ti-decorated BM exhibits better stability, dispersity, and chemical reactivity compared with other 2-dimensional materials. Our results suggest that the Ti-decorated BM monolayer will be a promising material system for hydrogen storage suggested by the DOE for commercial applications.

Acknowledgements

This work was supported by the National Natural Science Foundation of Shaanxi Province (Grant No. 2014JM2-5058), the Scientific Research Program of Yan'an (Grant No.2013-KG03), the Science Innovation Training Program (2014107191081), the Science Foundation of Yan'an University (YD2014-02) and the special Research funds for discipline construction of high level University.

Notes and references

- 1 P. C. Aeberhard, K. Refson, P. P. Edwards and W. I. F. David, Phys. Rev. B, 2011, **83**, 174102.
- 2 F. C. Zhang, Y. Liu and W. B. Zhang, Chinese Phys. Lett., 2015, **32**, 057302.
- 3 A. C. Dillon, Jones, K. M., Bekkedahl, T. A., C. H. Kiang, D. S. Bethune and M. J. Heben, Nature, 1997, **386**, 377-379.
- 4 S. S. Han, H. Furukawa, O. M. Yaghi and W. A. Goddard, J. Am. Chem. Soc., 2008, **130**, 11580-11581.

ARTICLE

Journal Name

- 5 S. S. Kaye and J. R. Long, *J. Am. Chem. Soc.*, 2005, **127**, 6506-6507.
- 6 C. Liu, Y. Y. Fan, M. Liu, H. T. Cong, H. M. Cheng and M. S. Dresselhaus, *Science*, 1999, **286**, 1127-1129.
- 7 Y. Ye, C. C. Ahn, C. Witham, B. Fultz, J. Liu and A. G. Rinzler, *Appl. Phys. Lett.*, 1999, **74**, 2307-2309.
- 8 H. Tang and S. Ismail-Beigi, *Phys. Rev. Lett.*, 2007, **99**, 115501.
- 9 X. J. Wu, J. Dai, Y. Zhao, Z. W. Zhuo, J. L. Yang and X. C. Zeng, *ACS Nano*, 2012, **6**, 7443-7453.
- 10 Y. Zhang, N. W. Franklin, R. J. Chen and H. J. Dai, *Chem. Phys. Lett.*, 2000, **331**, 35-41.
- 11 S. B. Fagan, A. Fazzio and R. Mota, *Nanotechnology*, 2006, **17**, 1154-1159.
- 12 S. Banerjee, S. Nigam, C. G. S. Pillai and C. Majumder, *Int. J. Hydrogen Energ.*, 2012, **37**, 3733-3740.
- 13 N. H. Song, Y. S. Wang, Q. Sun and Y. Jia, *Appl. Surf. Sci.*, 2012, **263**, 182-186.
- 14 Y. Liu, L. Ren, Y. He and H. P. Cheng, *J. Phys.: Condens. Matter*, 2010, **22**, 445301.
- 15 B. Delley, *J. Chem. Phys.*, 2000, **113**, 7756-7764.
- 16 B. Hammer, L. B. Hansen and J. K. Norskov, *Phys. Rev. B*, 1999, **59**, 7413-7421.
- 17 T. A. Halgren and W. N. Lipscomb, *Chem. Phys. Lett.*, 1977, **49**, 8.
- 18 T. Hirano, *MOPAC Manual*, in: J.J.P. Stewart (Ed.), Seventh ed., 1993.
- 19 D.G. Costa, A.B. Rocha and R. Diniz, *J. Phys. Chem. C*, 2010, **114**, 14133-14140.
- 20 H. Lee, J. Ihm and M. L. Cohen, S. G. Louie, *Phys. Rev. B*, 2009, **80**, 115412.
- 21 W. B. Liu, Y. Liu and R. G. Wang, *Appl. Surf. Sci.*, 2014, **296**, 204-208.
- 22 W. B. Liu, Y. Liu, R. G. Wang, L. F. Hao, D. J. Song and Z. Li, *Phys. Status Solidi. B*, 2014, **251**, 229-234.
- 23 J.L. Li, H.Y. Zhang and G.W. Yang, *J. Phys. Chem. C*, 2015, **119**, 19681-19688.

Table captions:**Table 1**

The Mulliken charge population of the layer in the $(\text{H}_2)_n/\text{Ti}/\text{BM}$ system, where the unit of the atom charge is one electron charge $|e|$, n is the number of the adsorbed H_2 .

Table 2

The adsorption energy (E_a), bond length ($r_{\text{H-H}}$), and Mulliken charge population of H_2 for more than one H_2 adsorbed on Ti/BM system, where the unit of the atom charge is one electron charge $|e|$.

Table 1

The Mulliken charge population of the layer in the $(\text{H}_2)_n/\text{Ti}/\text{BM}$ system, where the unit of the atom charge is one electron charge $|e|$, n is the number of the adsorbed H_2 .

Atom	BM	n=0	n=1	n=2	n=3	n=4	n=5
Ti	-	0.54	0.37	0.30	0.06	-0.34	-0.39
B1	-0.05	-0.01	-0.06	-0.05	-0.01	0.03	0.03
B2	0.16	0.28	0.03	0.03	0.07	0.14	0.15

Table 2

The adsorption energy (E_a), bond length ($r_{\text{H-H}}$), and Mulliken charge population of H_2 for more than one H_2 adsorbed on Ti/BM system, where the unit of the atom charge is one electron charge $|e|$.

Model	Ti	1 st H_2	2 nd H_2	3 rd H_2	4 th H_2	5 th H_2	E_a (eV/ H_2)	$r_{\text{H-H}}$ (Å)
Ti / BM	0.54							
$\text{H}_2/\text{Ti}/\text{BM}$	0.37	0.06					-0.47	0.81
$(\text{H}_2)_2/\text{Ti}/\text{BM}$	0.30	0.07	0.05				-0.36	0.82
$(\text{H}_2)_3/\text{Ti}/\text{BM}$	0.06	0.10	0.07	0.08			-0.26	0.80
$(\text{H}_2)_4/\text{Ti}/\text{BM}$	-0.34	0.12	0.12	0.10	0.09		-0.21	0.80
$(\text{H}_2)_5/\text{Ti}/\text{BM}$	-0.39	0.13	0.13	0.11	0.11	-0.02	-0.20	0.79

Figure captions:

Fig. 1. (a) The side view of BM: the triangular N pore ($H_{1,t}$), the hexagonal rings ($H_{2,t}$), the top of N1 ($N_{1,t}$), the top of N2 ($N_{2,t}$), and the top of C (C_t). (b) The top view of the BM and possible Ti decorating sites: the top of hexagonal rings ($H_{1,t}$), the top of B1 atoms ($B_{1,t}$), the top of B2 atoms ($B_{2,t}$), the top of bridge sites between B1 atoms (B_{r1}) and the top of bridge sites between B1 and B2 atoms (B_{r2}). The green and pink spheres denote B1 and B2 atoms, respectively.

Fig. 2. Calculated thermodynamic properties of pristine BM and Ti/BM material: (a) Enthalpy H , (b) heat capacity C_p , (c) Entropy S and (d) Gibbs free energy G .

Fig. 3 Illustrations of electron density distribution for (a) Ti/BM and (b) H_2 /Ti/BM systems. The (a') and (b') are the corresponding top views. The red, gray and green spheres denote Ti, C, and N atoms, respectively. The green and gray spheres denote B and Ti atoms, and the yellow spheres are the nearest B atoms beside Ti.

Fig. 4 The PDOS of the Ti/BM (a) before and (b) after H_2 adsorption. The Fermi energy is set to be 0 eV.

Fig. 5 Diffusion energy barrier as a function of diffusion coordinate and detailed diffusion pathway of the Ti atom on the BM, where IS, TS, and FS are the structure of the initial state, transition state, and the final state, respectively. (a) for the single Ti atom, a single Ti atom migrates from the $H_{1,t}$ position to its nearest neighboring one (b) one Ti atom migrating from the $H_{1,t}$ position to its secondary nearest neighboring $H_{1,t}$ position. The green and gray spheres denote B and Ti atoms, respectively.

Fig. 6 The relaxed adsorption of H_2 molecules on Ti/BM. (a) Side view of BM structure possibly adsorbing up to 18 Ti atoms on the both faces (b) Ti/BM structure adsorbing up to 80 H_2 on the double face, respectively. (a') and (b') are the top views corresponding to (a) and (b), respectively. The green, gray and white spheres denote B, Ti and H atoms, respectively.

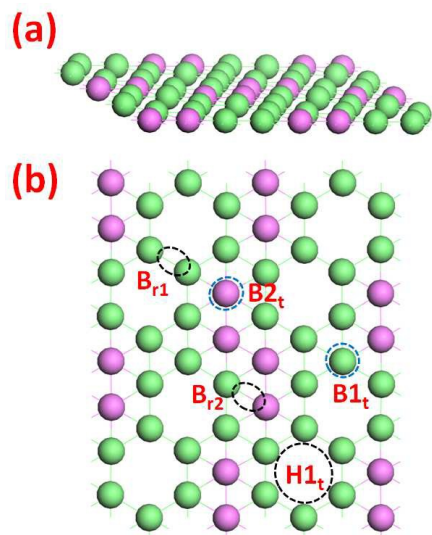


Fig. 1.(a) The side view of BM: the triangular N pore ($H1_t$), the hexagonal rings ($H2_t$), the top of N1 ($N1_t$), the top of N2 ($N2_t$), and the top of C (C_t). (b) The top view of the BM and possible Ti decorating sites: the top of hexagonal rings ($H1_t$), the top of B1 atoms ($B1_t$), the top of B2 atoms ($B2_t$), the top of bridge sites between B1 atoms (B_{r1}) and the top of bridge sites between B1 and B2 atoms (B_{r2}). The green and pink spheres denote B1 and B2 atoms, respectively.

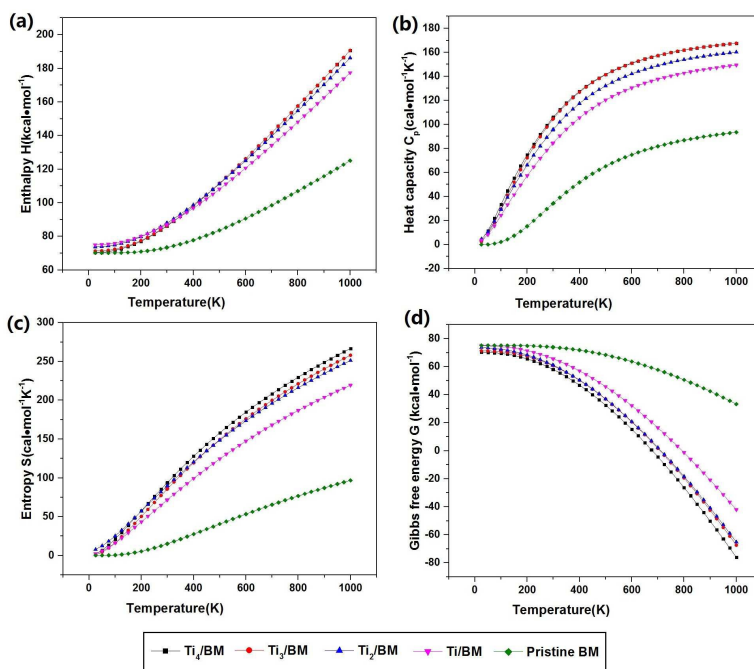


Fig. 2. Calculated thermodynamic properties of pristine BM and Ti/BM material: (a) Enthalpy H , (b) heat capacity C_p , (c) Entropy S and (d) Gibbs free energy G .

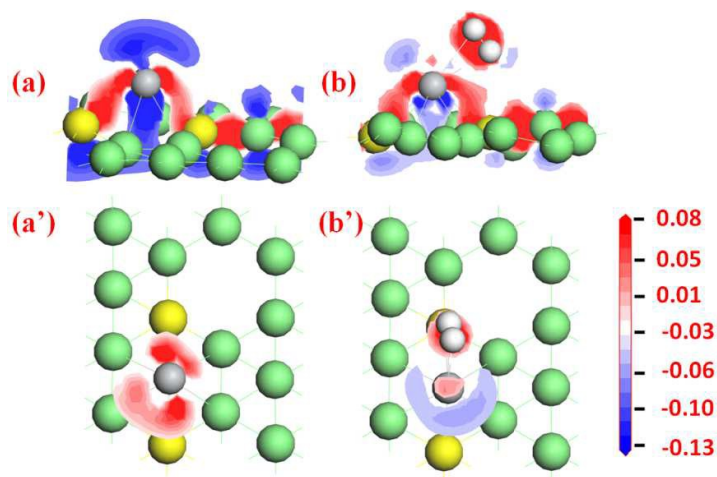


Fig. 3 Illustrations of electron density distribution for (a) Ti/BM and (b) H₂/Ti/BM systems. The (a') and (b') are the corresponding top views. The red, gray and green spheres denote Ti, C, and N atoms, respectively. The green and gray spheres denote B and Ti atoms, and the yellow spheres are the nearest B atoms beside Ti.

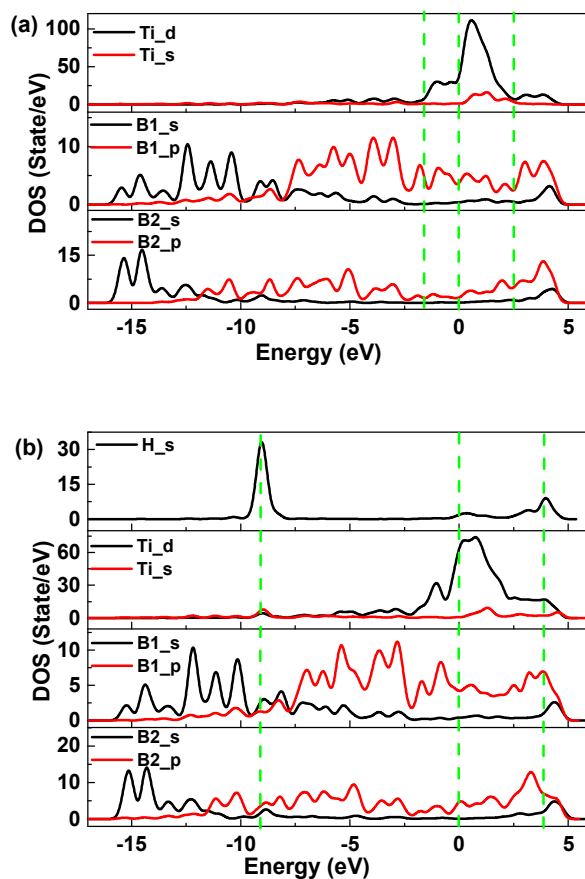


Fig. 4 The PDOS of the Ti/BM (a) before and (b) after H₂ adsorption. The Fermi energy is set to be 0 eV.

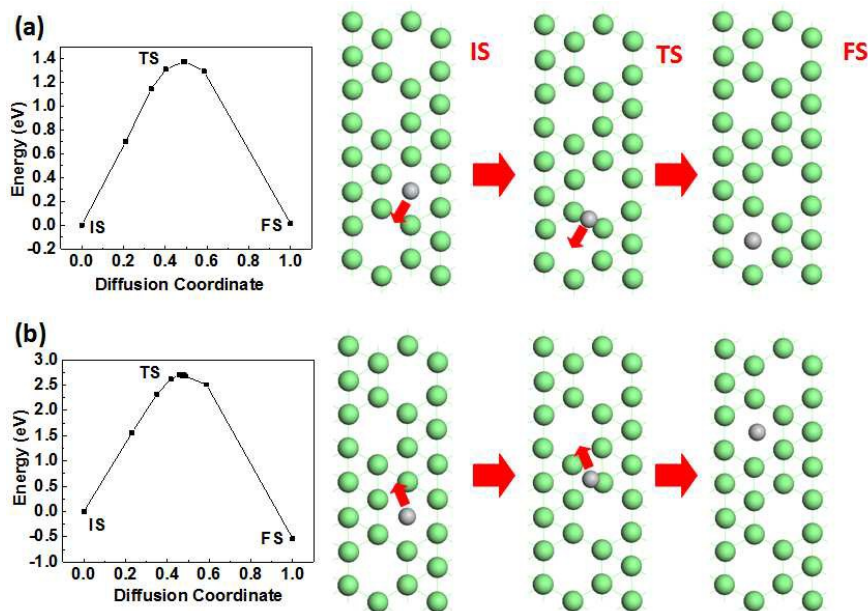


Fig. 5 Diffusion energy barrier as a function of diffusion coordinate and detailed diffusion pathway of the Ti atom on the BM, where IS, TS, and FS are the structure of the initial state, transition state, and the final state, respectively. (a) for the single Ti atom, a single Ti atom migrates from the H_{1t} position to its nearest neighboring one (b) one Ti atom migrating from the H_{1t} position to its secondary nearest neighboring H_{1t} position. The green and gray spheres denote B and Ti atoms, respectively.

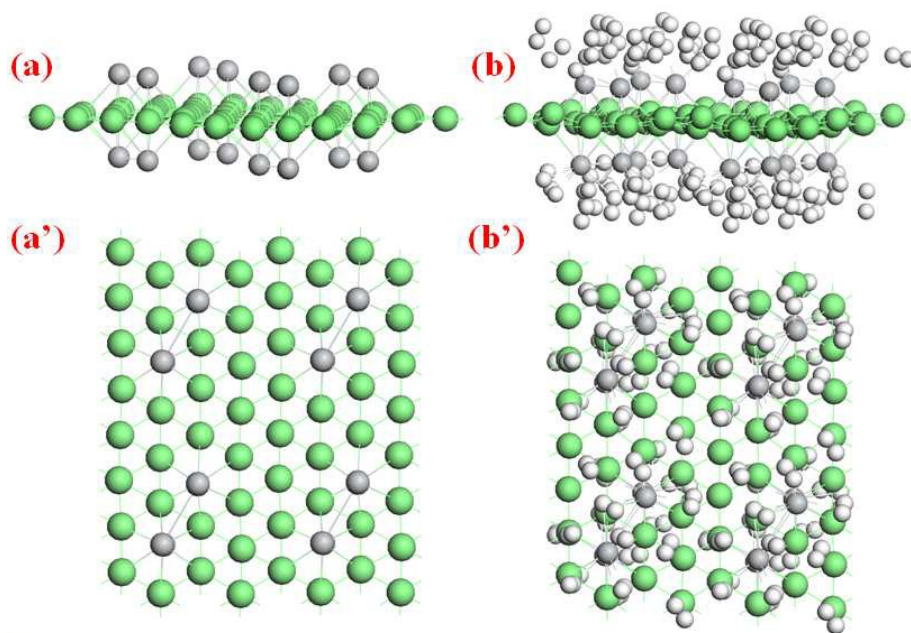


Fig. 6 The relaxed adsorption of H_2 molecules on Ti/BM. (a) Side view of BM structure possibly adsorbing up to 18 Ti atoms on the both faces (b) Ti/ BM structure adsorbing up to 80 H_2 on the double face, respectively. (a') and (b') are the top views corresponding to (a) and (b), respectively. The green, gray and white spheres denote B, Ti and H atoms, respectively.

A promising Ti-decorated boron monolayer (BM) system for hydrogen storage is proposed through the use of density functional theory. Our results suggest that the Ti-BM will be a promising material system for hydrogen storage.

